Catalysis Letters Vol. 108, Nos. 1–2, April 2006 (© 2006)
DOI: 10.1007/s10562-006-0026-x

Ni–Fe catalysts based on perovskite-type oxides for dry reforming of methane to syngas

Sania Maria de Lima* and José Mansur Assaf

Departamento de Engenharia Química, Universidade Federal de São Carlos, Rodovia Washington Luís Km 235, CEP 13565-905, São Carlos, SP, Brasil

Received 20 October 2005; accepted 7 January 2006

$LaNi_{(1-x)}Fe_xO_3$ ($x = 0$, 0.2, 0.4 and 0.7) perovskite-type catalysts were modified by the partial substitution of nickel by iron, aiming to increase the stability and resistance to carbon deposition during the methane dry reforming reaction. The results showed that a suitable combination of precipitation and calcination steps could result in oxides with the desired structure and with improved properties from the point of view of heterogeneous catalysis. The partial substitution of Ni by Fe in the perovskite structure resulted in decreasing rates of conversion of both reactants. However, the stability of the catalyst during the reaction was highly increased. These substituted catalysts were shown to be stable and the $LaNi_{0.8}Fe_{0.2}O_3$ catalyst, calcined at 800 °C for 5 h, was the most active in the reaction conditions.

KEY WORDS: Perovskite; dry reforming of methane; $La(Ni,Fe)O_3$; carbon deposition.

1. Introduction

Owing to the existence of large reserves of natural gas around the world, a lot of research focuses on the development of processes that generate gas to liquid hydrocarbons fuels (GTL) and valuable oxygenated chemicals from this raw material. The classical GTL route encloses both the synthesis gas generation from natural gas (methane) and the synthesis gas conversion to liquid fuels [1]. In these processes, the synthesis gas production section is considered to account for around 60% of the total capital cost [2,3]. Thus, the economical viability of this process relies strongly on the decrease of the costs of synthesis gas generation and alternative routes to syngas production can be considerate.

For many years, the steam reforming of methane has been a major line of production of synthesis gas (H_2/CO), a product of great industrial interest. Now, much research is in progress on methods that enable the reforming of methane with carbon dioxide, because the low H_2/CO ratio is more suitable for production of methanol and the Fischer–Tropsch synthesis [4]. As a bonus, this reaction also has an important environmental advantage in that both methane and carbon dioxide are greenhouse gases [5,6].

Studies of catalysts for the CO_2 reforming of methane have shown that noble metals such as Rh, Pt, Ru and Ir perform well [7–9]. Ni catalyst exhibits similar activity and selectivity to the noble metals, but is deactivated quickly, owing to carbon deposition [10]. However, because of the very high cost of noble metal catalysts, it would be desirable to develop an effective promoted Ni catalyst which exhibits both catalytic activity and resistance to coking in CO_2 reforming of methane. It is possible to favor this change by adding oxides of alkaline earth metals of high basicity to the metal-support system [11]. Hence, a new approach to catalyst preparation that results in the formation of well-dispersed and stable Ni metal particles on the surface should be investigated. Use of precursors with perovskite structure not only fulfils the stability requirements, but also, by reduction of the B-sites cations (see below) which are distributed in the structure, results in the formation of a well-dispersed and stable metal particle catalyst [12].

These oxides are represented by the general formula ABO_3 in which the A ions can be rare-earth, alkaline earth or alkali elements that fit into dodecahedral sites of the framework, while the B ions can be 3d, 4d and 5d transition metal ions, which occupy the octahedral sites, whose vertices are occupied by O^{2-}. Perovskites have a unique structure capable of accepting a wide range of substitutions [13]. These solids are very resistant to high temperatures and mechanically and chemically stable under typical reaction conditions [14]. Moreover, partial substitution at the A site can strongly affect catalytic activity through the stabilization of unusual oxidation states of the B component and the simultaneous formation of structural defects [15].

The interactions created by the formation of bonds between Ni oxide and rare earth permit to increase the reduction temperature of nickel oxide. However, particularly for $LaNiO_3$, the thermal stability of the perovskite is low under a reducing atmosphere and coke formation

* To whom correspondence should be addressed.
E-mail: psania@iris.ufscar.br

can still be important [16]. A study of $LaNi_{(1-x)}Fe_xO_3$ catalysts to obtain synthesis gas has shown that the addition of iron to the perovskite structure can stabilize the structure under test conditions and limit the mobility of the active nickel [17]. With the aim of stabilizing the perovskite structure under a reducing atmosphere and to test its efficiency in the CO_2 reforming of methane to produce of synthesis gas to the GTL process, the influence of preparation conditions and of the partial substitution of Ni by Fe in the $LaNi_{(1-x)}$ Fe_xO_3 structure were investigated in this study.

2. Experimental

2.1. Catalyst preparation

The catalyst precursors were prepared by discontinuous precipitation. An aqueous solution containing equimolar quantities of nitrates of La and Ni (with addition of nitrate of Fe in substituted catalysts) was quickly added to an aqueous solution of sodium carbonate (0.5 M) under continuous stirring. The precipitate formed was washed thoroughly with distilled water and filtered under vacuum to remove the remaining traces of ions and dried at 60 °C for 20 h. The product was ground, decomposed for 3 h at 550 °C in air and calcined under various conditions: 800 °C for 5 h, 900 °C for 5, 10 and 15 h, to observe the effects of calcining variables on the perovskite structure obtained and on the catalytic performance.

2.2. Catalyst characterization

The amounts of La, Ni and Fe in the compounds were measured by inductively-coupled plasma atomic emission spectroscopy (ICP-AES) in a VISTA-VARIAN spectrometer. The perovskite structure of all catalysts was confirmed by powder X-ray diffraction (XRD) using a Siemens D-5005 diffractometer with CuK_α radiation. The diffraction patterns were recorded in the range $2\theta = 5–80°$ at $2° \text{ min}^{-1}$. Crystalline phases were identified in the JCPDS database. The specific surface area of the catalysts was measured by the BET method by measuring the adsorption of nitrogen at −196 °C, using a Quantachrome Nova 1200 analyzer. Temperature programmed reduction (TPR) was carried out on a Micromeritics Pulse Chemisorb 2705, using 30 mg of sample placed in a U shaped quartz reactor with a heating rate of 10 °C min^{-1} from room temperature up to 1000 °C. The reducing gas used was a mixture of 5% H_2/N_2 with flowing at 30 mL min^{-1}. Thermogravimetric analysis (TGA) was performed on catalysts after the dry reforming stability tests in an analyzer TA Instruments SDT 2960 Simultaneous DSC-TGA, at a heating rate of 10 °C min^{-1}, from room temperature up to 900 °C, with synthetic air flow.

2.3. Catalytic activity measurements

The methane dry reforming reaction was carried out over 10 h at 650 °C and atmospheric pressure, in a fixed-bed quartz micro-reactor loaded with 100 mg catalyst, over while an equimolar mixture of CH_4 and CO_2 flowed continuously at 120 mL min^{-1}. The conditions used to reduce the samples, before the reaction, were established by observation of the results of TPR. The samples with $x = 0$ were reduced *in situ* at 700 °C for 4 h, $x = 0.2$ and 0.4 at 800 °C for 4 h and $x = 0.7$ at 860 °C for 4 h, with pure H_2 flowing at 40 mL min^{-1}. Products of reaction were analyzed in an on-line chromatograph gas (GC 3800, VARIAN), with two thermal conductivity detectors and columns packed with Porapak N and 13X Molecular sieves.

3. Results and discussion

3.1. Catalyst characterization

The nominal values and the results of the quantitative analysis by ICP-AES of lanthanum, nickel and iron are presented in Table 1. These values are expressed as percent weight of each component and show a good balance between the nominal and experimental values.

The XRD diagrams for the $LaNiO_3$ samples produced under various calcination conditions are shown in figure 1. The perovskite structure was identified as a single phase in all samples. The sample calcined at 800 °C belongs to the cubic system with space group Pm3m (221). On increasing the calcining temperature and the time, an increase in the crystallinity was observed with formation of a better-defined perovskite structure. This increased severity in the calcination conditions led to the conversion of the perovskite structure from the cubic phase to hexagonal (pattern shown in figure 1). This structure shift was before observed by Rakshit and Gopalakrishnan [18] that have synthesized $LaNiO_3$ perovskites and observed the perovskite structure as a single phase, with cubic structure and lattice parameter $a = 3.851$ Å, in samples calcined at 800 °C for 4 h. They found out that when the time of calcinations was increased at this same temperature, there was a gradual conversion from the cubic to

Table 1
Inductively coupled plasma atomic emission spectroscopy analyses (% weight)

Catalyst	Nominal %			Measured %		
	La	Ni	Fe	La	Ni	Fe
$LaNiO_3$	56.6	23.9	–	53.3	23.3	–
$LaNi_{0.8}Fe_{0.2}O_3$	56.7	19.2	4.5	52.8	18.7	4.1
$LaNi_{0.6}Fe_{0.4}O_3$	56.9	14.4	9.1	50.3	13.3	8.1
$LaNi_{0.3}Fe_{0.7}O_3$	57.1	7.2	15.9	50.8	6.7	15.1

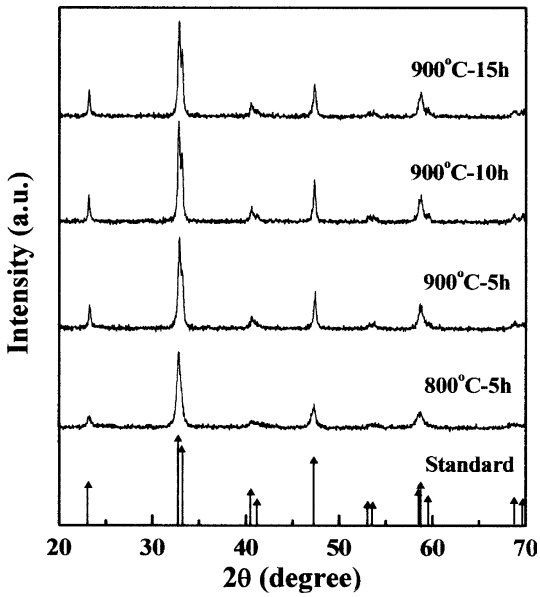

Figure 1. X-ray diffraction (XRD) patterns of $LaNiO_3$ perovskite oxides calcined under various conditions of temperature and time.

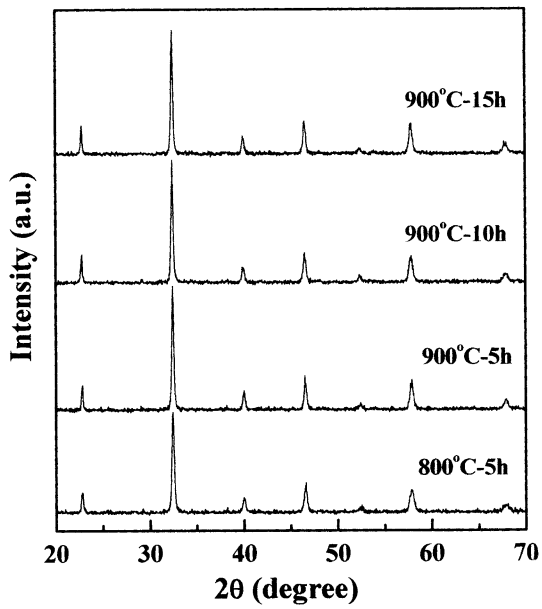

Figure 2. X-ray diffraction (XRD) patterns of $LaNi_{0.3}Fe_{0.7}O_3$ perovskite oxides calcined under various conditions of temperature and time.

the hexagonal phase, which involved a continuous but small loss of oxygen and a gradual increase in the axial angle α from 90° of the cubic phase to about 90°43′, going through a transient rhombohedral phase until complete transformation to the hexagonal phase. Thus, the perovskite calcined at 800 °C is closer to the cubic phase than hexagonal, undergoing transformation to the hexagonal phase on increasing the calcination temperature or time.

Comparing the catalysts substituted partially by Fe produced under different calcination conditions, an increase of crystallinity was seen for higher calcining temperatures and no significant change with increased time of calcination. The $LaNi_{0.3}Fe_{0.7}O_3$ sample was chosen to represent these results (figure 2).

There are no reference diagrams in the specialized literature of perovskite structures with the compositions studied here. In view of this, the XRD diagrams of the $LaNi_{(1-x)}Fe_xO_3$ series were compared to $LaNiO_3$ (hexagonal) and $LaFeO_3$ (orthorhombic) reference diagrams and, in each case, only one perovskite phase was obtained.

As the calcining temperature has a stronger influence in defining a perovskite structure than varying the time, a more detailed study with this series of catalysts was performed on the perovskites calcined at 800 °C for 5 h and at 900 °C for 10 h. In figure 3 are shown the XRD diagrams of the $LaNi_{(1-x)}Fe_xO_3$ ($x = 0$, 0.2, 0.4 and 0.7) catalysts calcined at 900 °C for 10 h, in which the effect of the partial substitution of nickel by iron can be seen. All the standard patterns are presented in the form of relative intensity I/I_0. A progressive and regular shift of the diffraction peaks to the left is observed when Ni is replaced by iron, accompanied of a small increase in

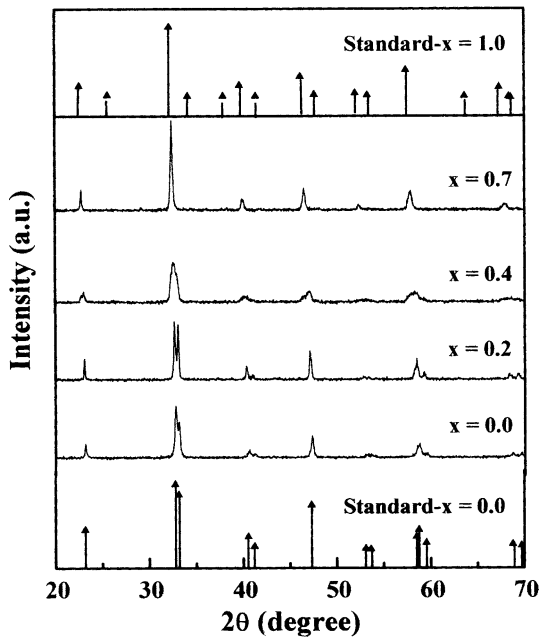

Figure 3. X-ray diffraction (XRD) patterns of $LaNi_{(1-x)}Fe_xO_3$ perovskite oxides calcined at 900 °C for 10 h.

their intensity (except for $x = 0.4$). This shift indicates the formation of a solid solution of $LaFeO_3$ and $LaNiO_3$ in all proportions [17]. A zoom on the 2θ diagram between 32.0 and 33.7 shows better this progressive shift in the most intensive diffraction peak of some $LaNi_{(1-x)}Fe_xO_3$ structures (figure 4).

Data showing the influence of partial substitution of Ni by Fe, under all calcination conditions, on the surface area of $LaNi_{(1-x)}Fe_xO_3$ perovskites are presented in figure 5. The perovskites, when synthesized from the

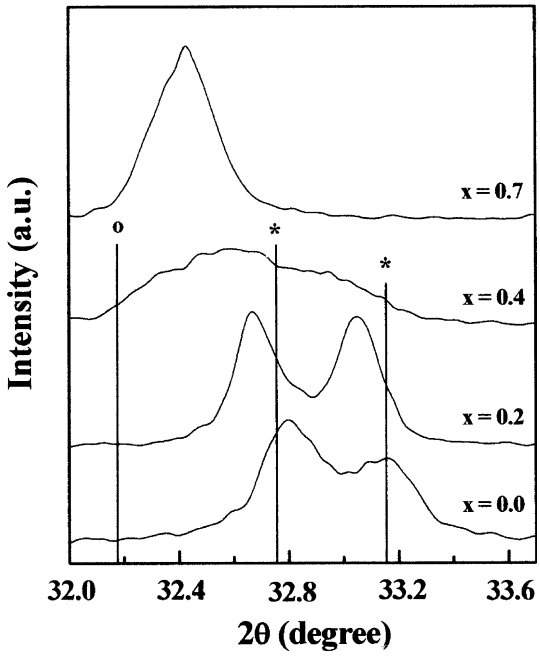

Figure 4. X-ray diffraction (XRD) highest peak of the $LaNi_{(1-x)}Fe_xO_3$ structures calcined at 900 °C for 10 h in the region 2θ between 32.0 and 33.7 with the reference phases (*) $LaNiO_3$ and (°) $LaFeO_3$.

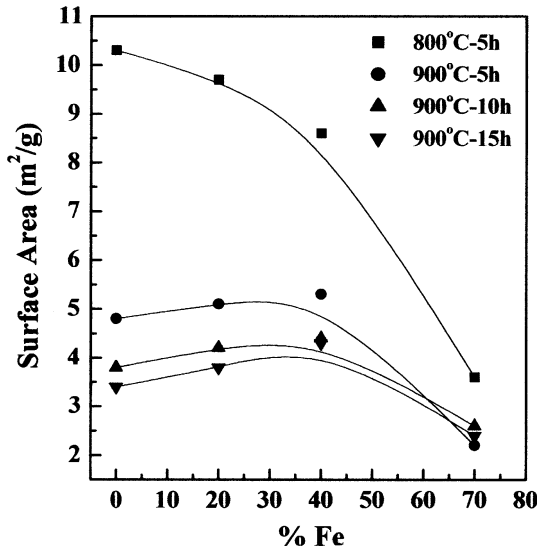

Figure 5. Surface area of $LaNi_{(1-x)}Fe_xO_3$ perovskite oxides.

component oxides at high temperatures by a solid-state reaction, exhibit low values of surface area (less than 5.0 $m^2\ g^{-1}$) [19]. It is observed that the partial substitution of nickel by iron results in decreasing of values of specific surface area (figure 5). Moreover, increasing the calcining temperature causes a significant fall in the values of surface area, this effect becoming more accentuated with increasing content of iron in the structure. On the other hand, varying the calcining times (5, 10 and 15 h) at the temperature of 900 °C, did not result in large alterations in texture.

The temperature programmed reduction analyses were carried out on all the oxides prepared. Their behavior in reducing atmosphere did not change significantly with the time of calcination. Therefore, only the TPR profiles of $LaNiO_3$ catalyst are presented, for all calcination conditions (figure 6). This perovskite showed two reduction peaks: the first corresponds to the formation of the $La_2Ni_2O_5$ structure, in other words, it results from the reduction of Ni^{3+} to Ni^{2+}, and the second corresponds to the reduction of Ni^{2+} to Ni^0, which remains deposited on lanthanum oxide [20]. It is seen that, on varying the calcining time, these peaks did not shift significantly in the reduction temperatures. The differences are more evident when the areas under the peaks are considered. These are proportional to the hydrogen consumption for reduction of the ions Ni^{+3} to Ni^{+2} (1st peak) and of Ni^{2+} to Ni^0 (2nd peak). Ideally, the area under this second peak should be double that of the first. The deviations from this ideal relationship, greatest for the sample calcined at 800 °C (5 h) and decreasing with increasing time of calcination at 900 °C, indicate the reduction of other components that were not observed by XRD and that contribute to hydrogen consumption.

It is possible, mainly under the mildest calcination conditions, that NiO and La_2O_3 were formed, besides the $LaNiO_3$ perovskite. This NiO can be reduced to Ni^0 simultaneously with the formation of $La_2Ni_2O_5$, resulting in hydrogen consumption (1st peak) larger than the expected. It can be said that the closer to 2.0 is the ratio 2nd peak area peak area: 1st peak area, the lower is the amount of compounds other besides of the structure perovskite.

The TPR profiles of the $LaNi_{(1-x)}Fe_xO_3$ ($x = 0$, 0.2, 0.4 and 0.7) oxides calcined at 800 °C for 5 h and 900 °C

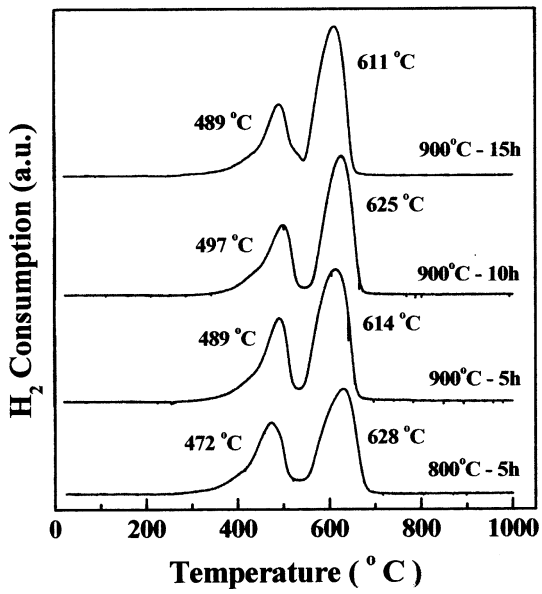

Figure 6. TPR profiles of $LaNiO_3$ perovskite oxides calcined under various conditions of temperature and time.

for 10 h are shown in figure 7. $LaFeO_3$ ($x=1$) is practically unreduced in these TPR conditions [17]. It is possible to see clearly that the first reduction peak is similar for all oxides containing nickel; even the temperature of maximum hydrogen consumption suffered only small variations as the amount of Ni decreased. However, the area under this peak decreased with decreasing Ni content, indicating that only the nickel was suffering reduction at this temperature. The temperature of the second peak, however, shifts from 625 °C ($LaNiO_3$) up to approximately 1000 °C ($LaNi_{0.3}Fe_{0.7}O_3$), with rising values of x. During this second reduction step, the nickel and part of the iron are reduced to metals and form a Ni–Fe alloy that comes as a more stable compound [17]. Provendier *et al.* [21] confirmed these TPR results by *in situ* magnetization and Mössbauer spectroscopy.

The temperatures of maximum hydrogen consumption for the second reduction peak increase with the addition of iron to the structure, indicating that nickel-poor catalysts are more stable under reducing conditions than nickel-rich ones. This shows the stabilizing effect of iron in the structure under these conditions.

When comparing the temperature of calcinations, it was observed that the structures obtained at 900 °C were a little more stable than those obtained at 800 °C, because the reduction peaks suffered a shift to the right.

After analyzing the results of TPR profiles for all catalysts, together with the XRD and surface area results, it was decided to carry out the catalytic tests with the samples calcined at 800 °C for 5 h and at 900 °C for 10 h, because as discussed previously, varying the time of calcination did not have a significant influence on the properties of reduction of the catalysts.

3.2. Catalytic activity measurements

From experimental data obtained from GC analysis of the products leaving the reactor, methane conversion (X_{CH_4}) and carbon dioxide conversion (X_{CO_2}) were plotted as a function of reaction time, to evaluate stability. The stability tests continued for approximately 10 h uninterrupted.

Results of the stability tests over $LaNiO_3$ catalyst calcined at 800 °C for 5 h and at 900 °C for 10 h are summarized in figure 8. Although their conversion rates were high, these catalysts were not stable, it being necessary to interrupt the reaction after 2.5 h for the catalyst calcined at 800 °C and after 1.20 h for that calcined at 900 °C, due to the rising pressure-drop in the reactor impeding the passage of the reactants, as a consequence of coke formation on the catalyst surface.

Results of the stability tests for $LaNi_{(1-x)}Fe_xO_3$ ($x=0.2$, 0.4 and 0.7) catalysts are summarized in figures 9 and 10. Substitution of Fe in the perovskite structure resulted in greater stability to catalyst deactivation, while causing a decrease in the catalytic activity.

Comparing figure 9a and 9b, it can also be observed that in all cases the CO_2 conversion was found to be higher than the CH_4 conversion (except with Fe0.4–900 and Fe0.7–800). This occurs because the reverse water-gas shift (RWGS) reaction, which is thermodynamically possible at 650 °C and also consumes CO_2 (reaction 1), occurs simultaneously with CO_2 reforming of CH_4. For this reason, the H_2/CO ratio always attains values lower than unity.

$$CO_2 + H_2 \rightarrow CO + H_2O. \quad (1)$$

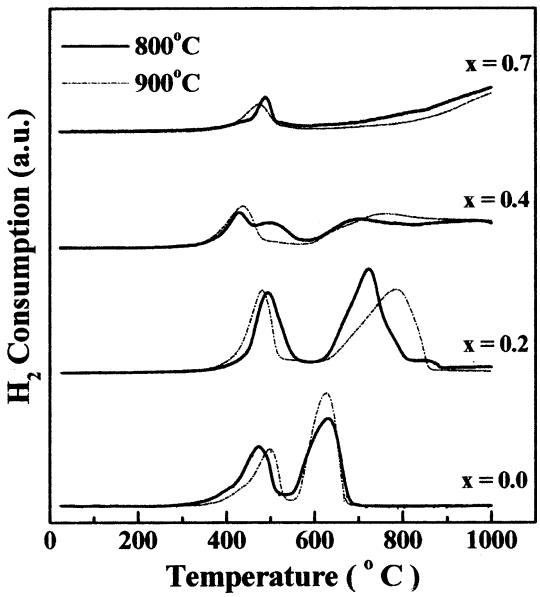

Figure 7. TPR profiles of $LaNi_{(1-x)}Fe_xO_3$ perovskite oxides calcined at 800 °C for 5 h and 900 °C for 10 h.

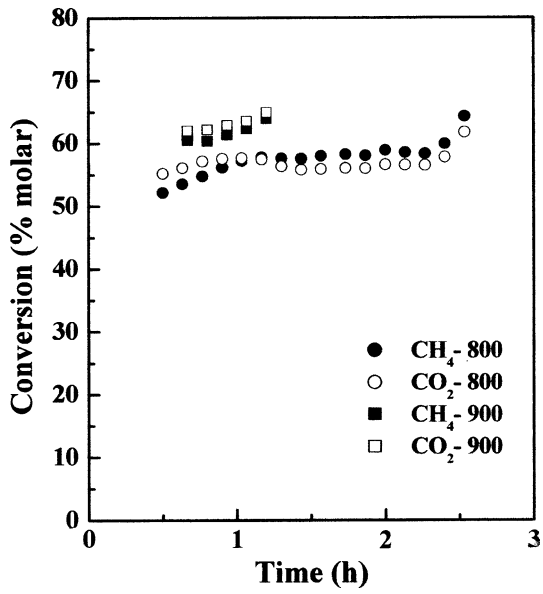

Figure 8. CH_4 and CO_2 conversion as a function of reaction time for $LaNiO_3$ perovskite oxides calcined at 800 °C for 5 h and 900 °C for 10 h.

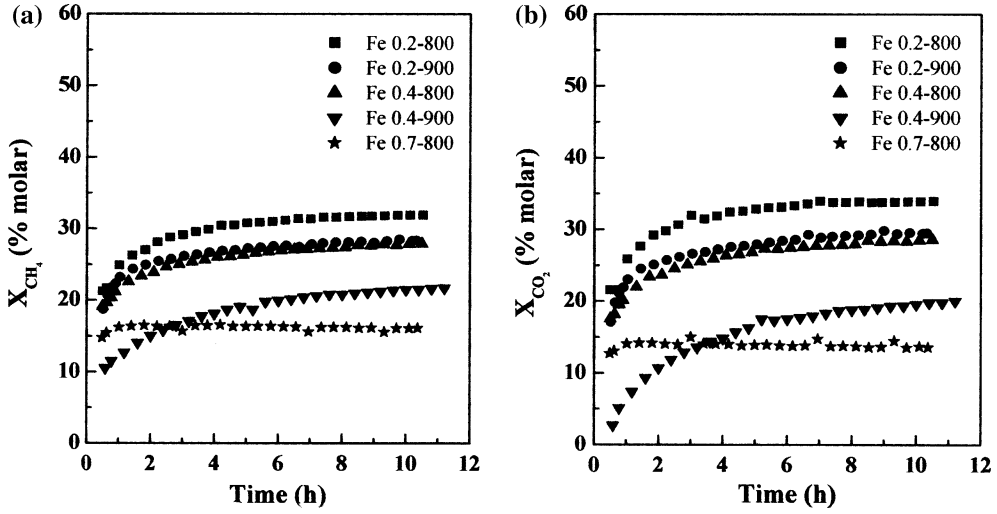

Figure 9. (a) CH_4 conversion and (b) CO_2 conversion as a function of reaction time for $LaNi_{(1-x)}Fe_xO_3$ perovskite oxides.

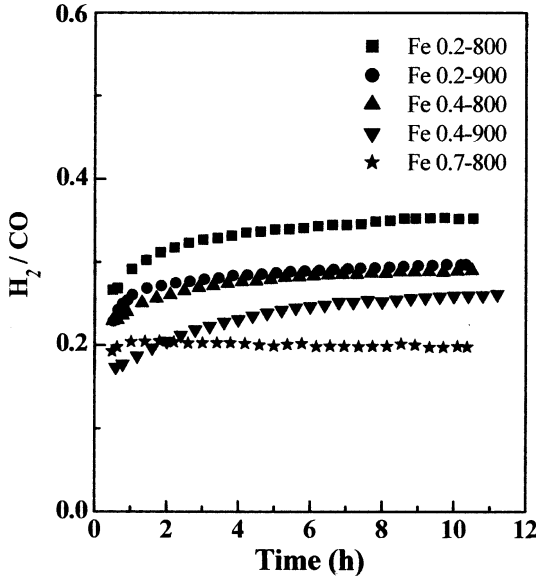

Figure 10. H_2/CO ratio as a function of reaction time for $LaNi_{(1-x)}Fe_xO_3$ perovskite oxides.

In relation to the calcining temperature, it was observed that the samples calcined at 800 °C showed higher values of conversion than those calcined at 900 °C. This fall in the catalytic activity with a higher calcining temperature can be explained by the surface area data that are greater for the samples calcined at 800 °C (figure 5). Analyzing the methane conversion or carbon dioxide conversion per unit surface area as a function of the reaction time (figures not shown), it was observed that all catalysts gave the same values of conversion, verifying that the number of sites of metallic Ni exposed on the surface are directly proportional to the surface area of the catalyst.

The $LaNi_{0.3}Fe_{0.7}O_3$ perovskite calcined at 900 °C for 10 h was not active for the tested reaction. This result is in agreement with published results [21], in which it was observed for $LaNi_xFe_{(1-x)}O_3$ catalysts with $x \leq 0.1$ that the iron alone is not very active in catalyzing the dry reforming of methane (CO_2 conversion and CH_4 conversion of 23% and 11%, respectively, for the $LaFeO_3$ catalyst at 800 °C), due to the low content of iron reduced in these reaction conditions.

$LaNi_{0.8}Fe_{0.2}O_3$ catalyst calcined at 800 °C for 5 h was both stable and the most active in reaction conditions, indicating that low contents of Fe in the Ni perovskite are sufficient to increase the stability of catalyst.

The amount of carbon deposited on the catalyst during the stability test was determined by thermogravimetric analysis with an oxidizing atmosphere. The curves presented in figure 11 show that the $LaNiO_3$ deactivation (figure 8) was caused by carbon deposition on catalyst surface and that the perovskite structure with iron can resist coke formation. The temperature of carbon gasification (600 °C) suggests that it was of the filamentous type.

The initial La–Ni–Fe perovskite permits a significant delay in the nickel reduction, especially when the amount of nickel in the structure is low. XRD analyses (figure not shown) of the catalysts after the catalytic test showed that, in all the samples, the perovskite structure was not maintained. Similar results was presented by Provendier *et al.* [21] with $LaNi_xFe_{(1-x)}O_3$ catalysts for dry reforming of methane: Ni and NiO deposited on La_2O_3 were found by XRD in the initially Ni-rich perovskites ($x = 1.0$ and 0.9), following the reactor test [21]. For $0.2 \leq x \leq 0.7$, part of the structure was present as a $LaFeO_3$ perovskite, and La_2O_3 and metallic nickel were also observed. However, in this case, there was evidence of Ni–Fe alloy formation during the test, which has not been observed in the catalysts proposed in literature. The presence of this alloy, which can modify the nickel

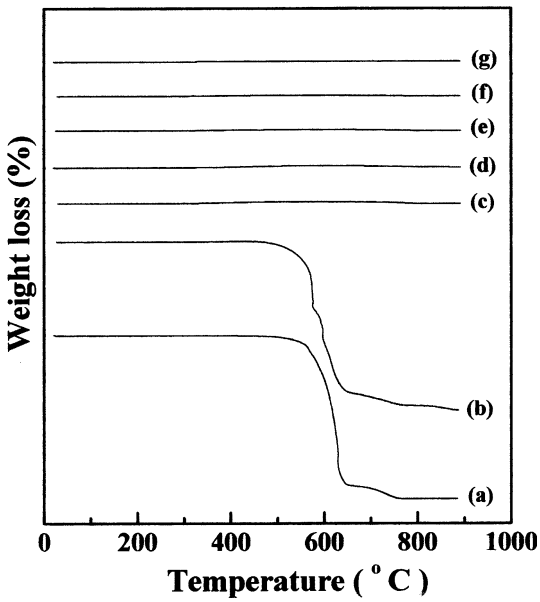

Figure 11. Thermogravimetric analysis for the $LaNi_{(1-x)}Fe_xO_3$ catalysts after 10 h of reaction. (a) Fe 0–800; (b) Fe 0–900; (c) Fe 0.2–800; (d) Fe 0.2–900; (e) Fe 0.4–800; (f) Fe 0.4–900, and (g) Fe 0.7–800.

particles on the surface of the catalyst, and the possible dilution of the active nickel sites as a consequence of the presence of iron, act to stabilize the perovskite structure that prevents the carbon formation.

In steam reforming [22], it was suggested that the key to coke formation is the nickel metal particle size and the interaction of nickel with the bi- or tri-metal perovskite structure. During regeneration tests on used catalysts, it was confirmed that in the nickel-poor systems, the presence of nickel within the perovskite network favors the formation of small nickel particles on the surface, thus preventing coking and improving the stability of the $LaNi_xFe_{(1-x)}O_3$ catalysts.

$LaNi_{(1-x)}Fe_xO_3$ systems, after the dry reforming of methane reaction were shown to contain metallic Ni, $LaFeO_3$ and La_2O_3 [21]. Hence, another possible explanation for the good stability of this system is that the presence of $LaFeO_3$ and lanthanum oxide in the reaction atmosphere can give an oxidizing character to the neighbourhood of the nickel particles and so contribute to the destabilization of the carbonaceous species on the active nickel sites.

4. Conclusions

The precipitation, a relatively simple method for catalysts preparation, can result in the desired perovskite structure. The XRD diffraction analyses showed that, already at 800 °C, some of the desired structure was formed, which became slightly more crystalline at longer times and higher temperatures of calcination and closer to the hexagonal phase. The synthesis of the perovskite-type oxides at 800 °C led to greater surface area than at 900 °C and the catalytic tests showed that these samples with larger surface area proved more active for conversion of reactants into products.

The substitution of Ni by Fe resulted in formation of a solid solution in all proportions and a decrease of the area under the first reduction peak (TPR) was observed, indicating that only the Ni was suffering reduction at this temperature. The temperature of reduction of the second peak increased with the addition of iron, indicating that Ni-poor catalysts are more stables under reducing conditions that Ni-rich ones.

$LaNiO_3$ catalysts calcined at 800 °C for 5 h and calcined at 900 °C for 10 h presented high initial catalytic activity, but suffered deactivation in the first hours of reaction, due to coke formation. Of the substituted catalysts, the $LaNi_{0.8}Fe_{0.2}O_3$ oxide calcined at 800 °C for 5 h was the most active in the reaction conditions, also showing that low contents of Fe are sufficient to promote stability for the catalyst. The catalysts calcined at 800 °C were shown to be more actives in the reaction conditions than those calcined at 900 °C, because of the higher values of surface area, the metallic Ni sites exposed on the surface being directly related to the surface area of the catalyst.

Acknowledgments

We gratefully acknowledge the CNPq (Brazil) to funding this work (project 473598/04-3); S.M. de Lima also acknowledges a fellowship granted to support of research for doctorate.

References

[1] K. Asami, X. Li, K. Fujimoto, Y. Koyama, A. Sakurama, N. Kometani and Y. Yonezawa, Catal. Today 84 (2003) 27.
[2] P.J. Lakhapate and V.K. Prabhu, Chem. Eng. World 35 (2000) 77.
[3] Oil Gas J. 15 (June) (1998) 34.
[4] E. Ruckstein and Y.H. Hu, Appl. Catal. A 154 (1997) 185.
[5] P. Chen, H. Zhang, G. Lin and K. Tsai, Appl. Catal. A 166 (1998) 343.
[6] C. Quincoses, A. Vargas, M. Montes, M. Gonzáles, in: Anais do XVI Simpósio Iberoamericano de Catálisis, Colombia (1998) 507.
[7] J.T. Richardson and S.A. Paripatyadar, Appl. Catal. 61 (1990) 293.
[8] A.T. Ashcroft, A.K. Cheetman, M.L.H. Green and P.D.F. Vernon, Nature 352 (1991) 225.
[9] F. Solymosi, G. Kutsan and A. Erdöhelyi, Catal. Lett. 11 (1991) 149.
[10] J.W. Nam, H. Chae, S.H. Lee, H. Jung and K.Y. Lee, Stud. Surf Sci. Catal. 119 (1998) 843.
[11] E. Ruckenstein and Y.H. Hu, Appl. Catal. A 133 (1995) 149.
[12] M.R. Goldwasser, M.E. Rivas, E. Pietri, M.J. Pérez-Zurita, M.L. Cubeiro, L. Gingembre, L. Leclercq and G. Leclercq, Appl. Catal. A 255 (2003) 46.
[13] L.G. Tejuca, J.L.G. Fierro and J.M.D. Tascón, in *Structure and Reactivity of PerovskiteType Oxides*, D.D. Eley, H. Pines and P.B. Weisz, eds. (Academic Press, New York), Adv. Catal. 36 (1989) 237.

[14] M.R. Goldwasser, E. Pietri, A. Barrios, O. Gonzáles, M.J. Pérez-Zurita and M.L. Cubeiro, in: Actas do XVII Simpósio Ibero-Americano de Catálise, Porto, Portugal (2000) 51.
[15] H. Falcón, J.A. Barbero, J.A. Alonso, M.J. Martinez-Lope and J.L.G. Fierro, Chem. Mater. 14 (2002) 2325.
[16] A. Slagtern and U. Olsbye, Appl. Catal. A 110 (1994) 99.
[17] H. Provendier, C. Petit, C. Estournès, S. Libs and A. Kiennemann, Appl. Catal. A 180 (1999) 163.
[18] S. Rakshit and P.S. Gopalakrishnan, J. Solid State Chem. 110 (1994) 28.
[19] P. Porta, S. de Rossi, M. Faticanti, G. Minelli, I. Pettiti, L. Lisi and M. Turco, J. Solid State Chem. 146 (1999) 292.
[20] S.M. de Lima, *Preparação e caracterização de perovskitas* $LaNi_{(1-x)}Fe_x O_3$ *e* $LaNi_{(1-x)} Co_x O_3$ *para a reforma do metano corn* CO_2 (Dissertação de Mestrado, São Carlos-SP, DEQ-UFSCar, 2002).
[21] H. Provendier, C. Petit, C. Estournès and A. Kiennemann, Stud. Surf. Sci. Catal. 119 (1998) 741.
[22] H. Provendier, C. Petit, C. Estournès and A. Kiennemann, Comptes Rendus de I'Academie des Sciences Series lie Chemitry 4 (2001) 64.